Electronic Supplementary Material (ESI) for Journal of Materials Chemistry B.

Supplementary Information

Development of a selective cell capture and release assay: impact of clustered RGD ligand

M. Degardin,[a] D. Thakar,[a] M. Claron,[a] R. P. Richter,[b,c,d] L. Coche-Guérente[a]* and D. Boturyn[a]*

[a] Univ. Grenoble-Alpes, CNRS, DCM UMR 5250, F-38000 Grenoble, France.
E-mail: didier.boturyn@univ-grenoble-alpes.fr

[b] University of Leeds, School of Biomedical Sciences and School of Physics and Astronomy, Leeds, United Kingdom.

[c] CIC biomaGUNE, Biosurfaces Lab, San Sebastian, Spain.

[d] Univ. Grenoble-Alpes, CNRS, LIPhy UMR 5588, F-38000 Grenoble, France.

Table of Contents

1. Materials and methods for HPLC, QCM-D and SE

1.1 HPLC methods

RP-HPLC analyses were performed on Waters equipment consisting of a Waters 600 controller, a Waters 2487 Dual Absorbance Detector and a Waters In-Line Degasser (Saint-Quentin-en-Yvelines, France). The analytical column used was a Nucleosil 120 Å 3 µm C18 particles, 125 × 4 mm operated at 1 mL/min with linear gradient programs in 20 min run time (routine program: 5% to 100 % B in 20 min). UV monitoring was performed most of the time at 214 nm and 250 nm simultaneously. Solvent A consisted of H_2O containing 0.1% TFA and solvent B consisted of CH_3CN containing 9.9% H_2O and 0.1% TFA. Water was of Milli-Q quality. CH_3CN and TFA were of HPLC use quality.

RP-UHPLC analyses were performed on Waters equipment consisting of a Waters Acquity H-Class Bio UPLC combined to a Waters SQ Detector 2 mass spectrometer. The analytical column used was a ACQUITY UPLC BEH C18 Column, 130 Å, 1.7 µm, 2.1 mm x 50 mm operated at 0.6 mL/min with linear gradient programs in 2.20 min run time (routine program: 5% to 100 % B in 2.20 min). UV monitoring was performed at 214 nm. Solvent A consisted of H_2O containing 0.1% formic acid (FA) and solvent B consisted of CH_3CN containing 0.1% FA. Water was of Milli-Q quality. CH_3CN and FA were LC-MS grade.

RP-HPLC purifications were either performed on Gilson GX-281 (high quantities: hundreds of mg) or GX-271 equipment (low quantities: few mg). For GX-281, the preparative column, Macherey-Nagel 100 Å 7 µm C18 particles, 250 × 21 mm was operated at 20.84 mL/min. For GX-271, the preparative column, Macherey-Nagel 300 Å 7 µm C18 particles, 250 × 10 mm (Hoerdt, France) was operated at 4.65 mL/min. Linear gradient programs in 30 min run time were used and solvents A and B were the same as the ones used in RP-HPLC analysis.

Electron spray ionization (ESI-MS) mass spectra were recorded on an Esquire 3000 (Bruker) spectrometer (Champs-sur-Marne, France). The multiply charged data produced by the mass spectrometer on the m/z scale were converted to the molecular weight.

2. HPLC profiles and MS analysis

2.1 Cyclopeptide 6

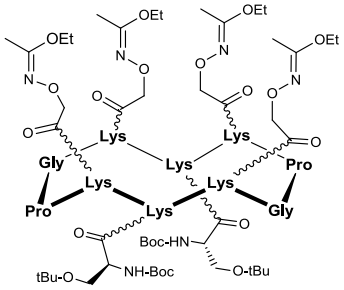

RP-HPLC profile and ESI-MS analysis of crude 6

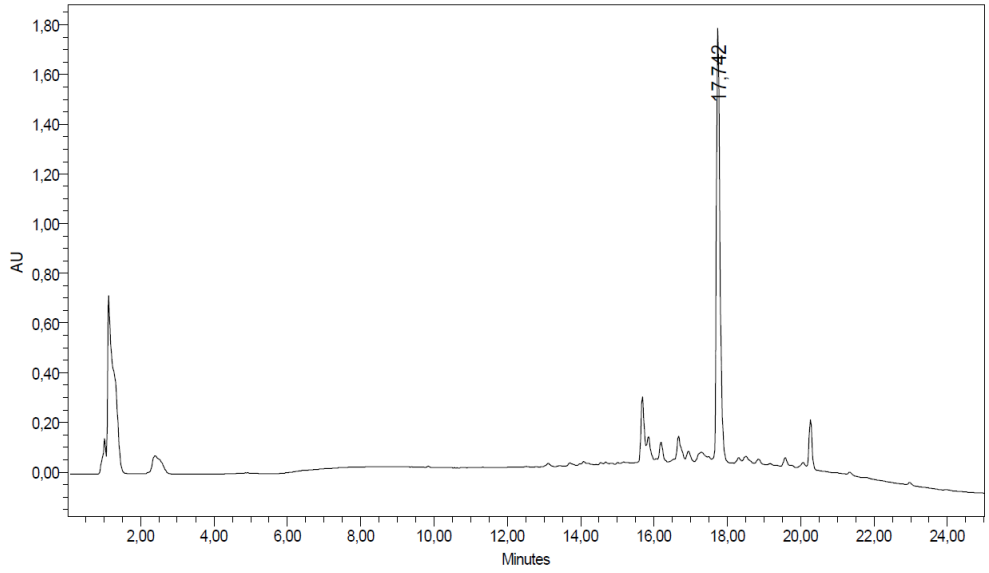

Figure S1: RP-HPLC profile of crude **6**.

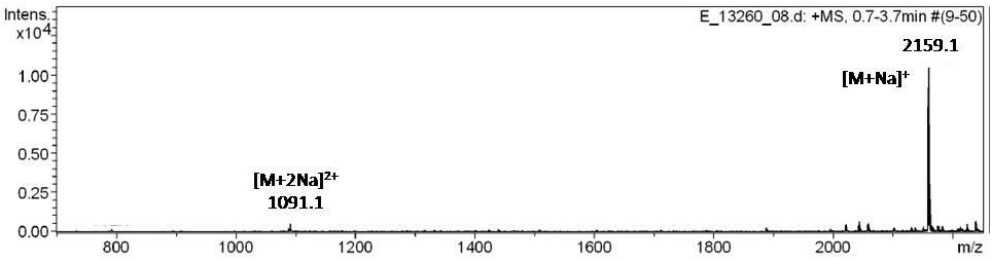

Figure S2: ESI-MS analysis of crude **6**.

Mass spectrum (ESI, positive mode) calculated mass for $C_{98}H_{170}N_{22}O_{30}$: 2136.3; found: 2136.1.

2.2 Cyclopeptide 8

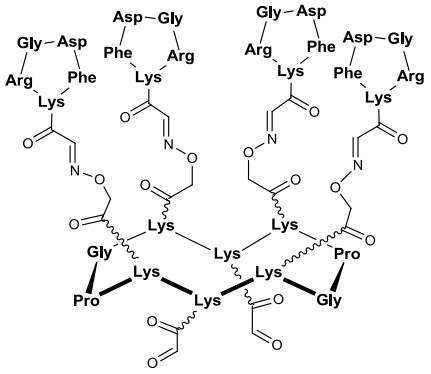

RP-HPLC profile and ESI-MS analysis of 8

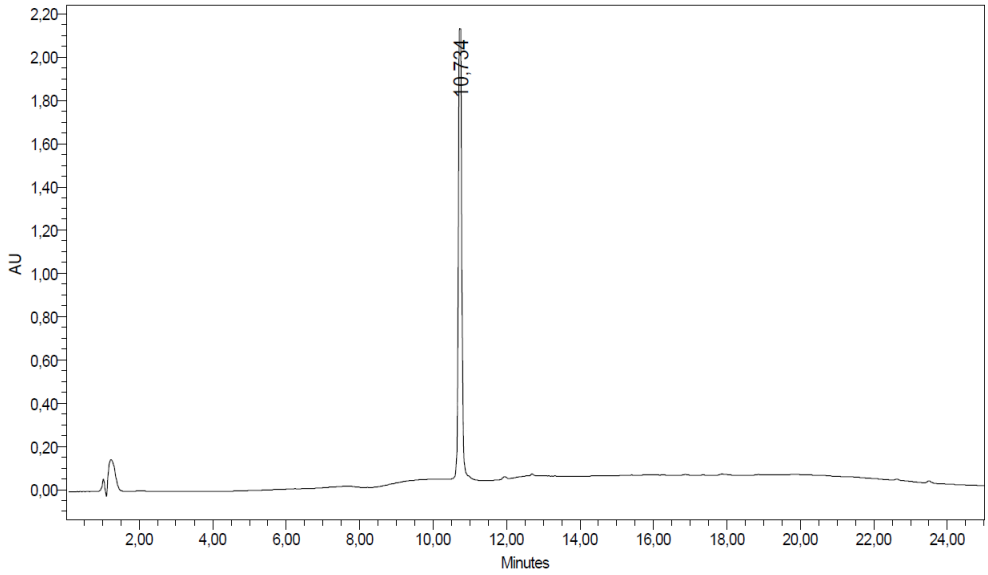

Figure S3: RP-HPLC profile of **8**.

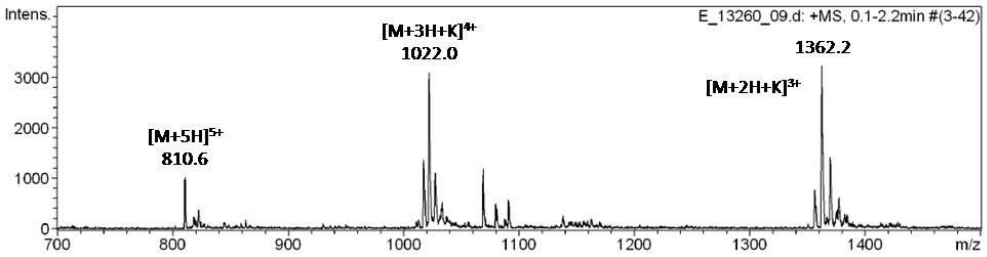

Figure S4: ESI-MS analysis of **8**.

Mass spectrum (ESI, positive mode) calculated mass for $C_{178}H_{260}N_{56}O_{54}$: 4048.3; found: 4049.2.

2.3 Cyclopeptide 7

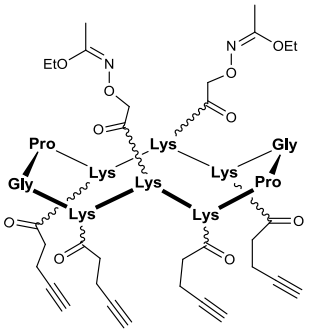

RP-HPLC profile and ESI-MS analysis of crude 7

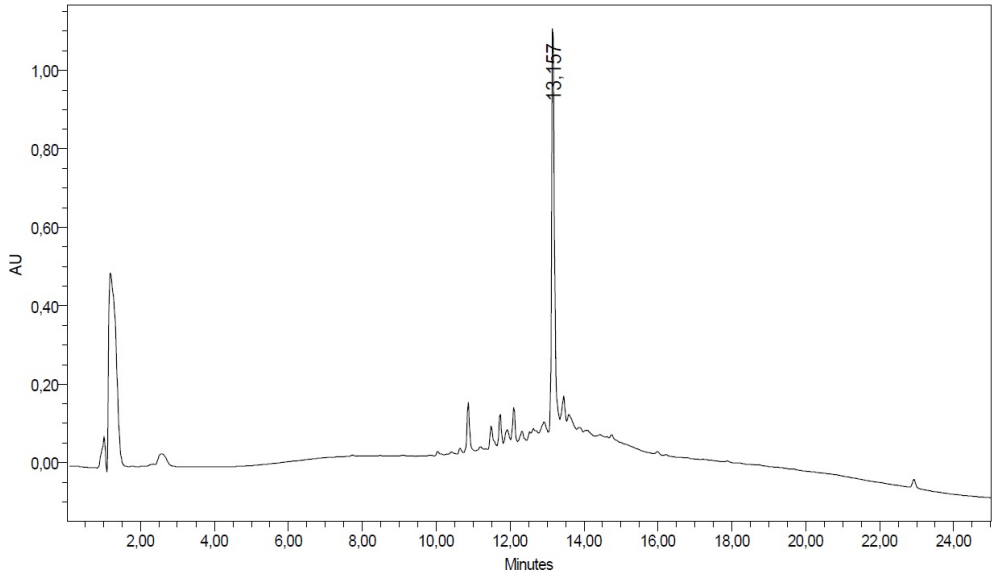

Figure S5: RP-HPLC profile of crude **7**.

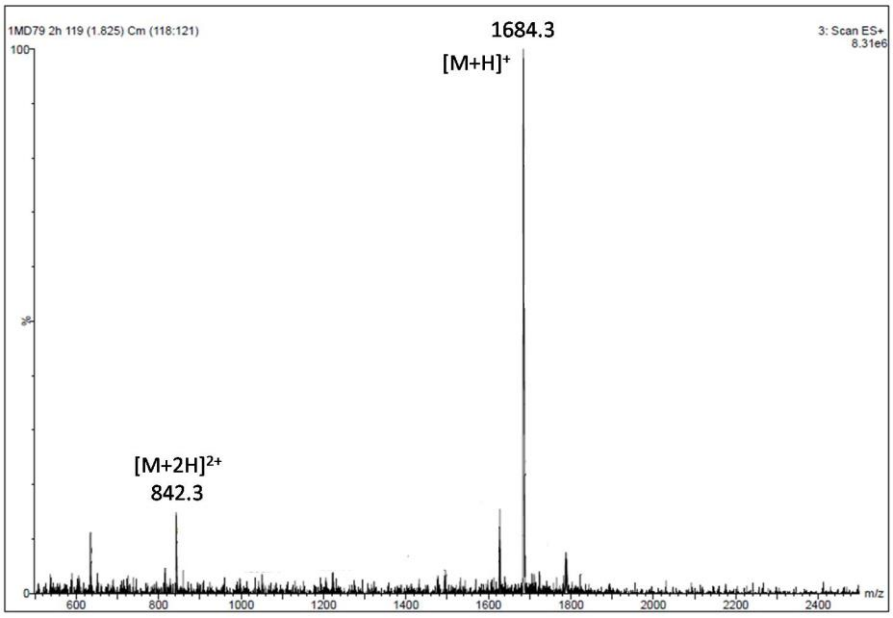

Figure S6: ESI-MS analysis of crude **7**.

Mass spectrum (ESI, positive mode) calculated mass for $C_{82}H_{126}N_{18}O_{20}$: 1682.9; found: 1683.3.

2.4 Conjugate 9

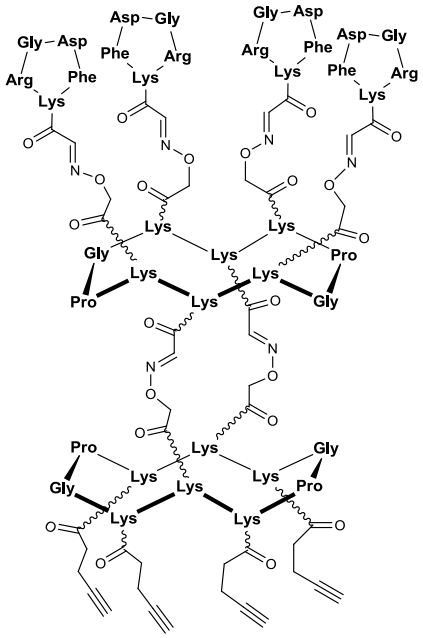

RP-HPLC profile and ESI-MS analysis of 9

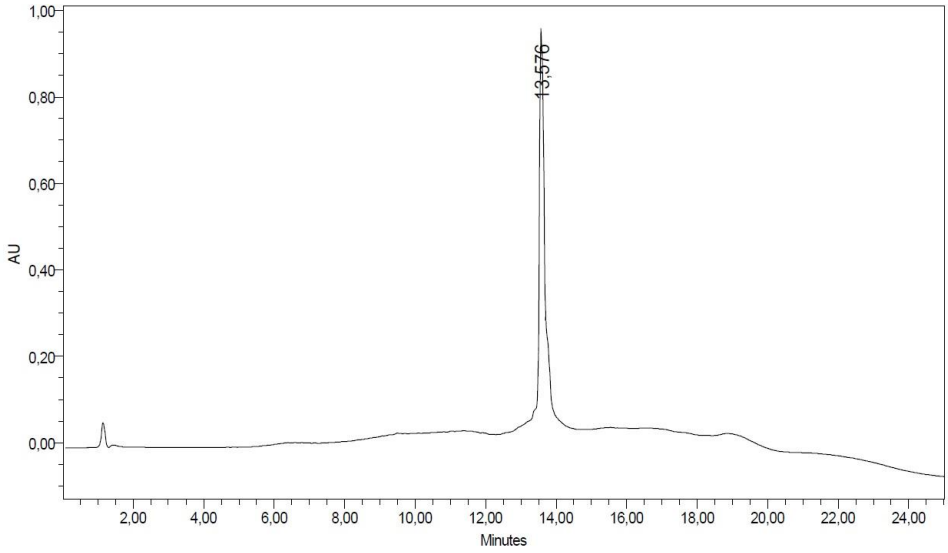

Figure S7: RP-HPLC profile of **9**.

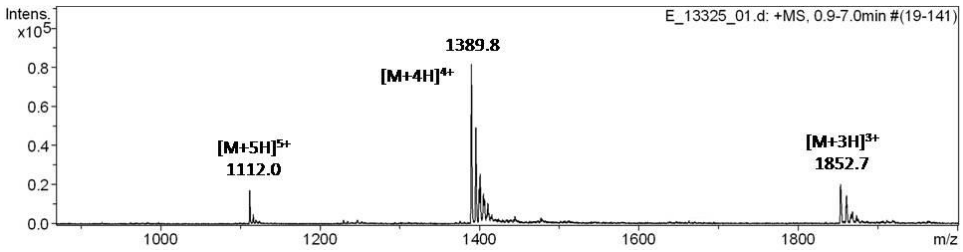

Figure S8: ESI-MS analysis of **9**.

Mass spectrum (ESI, positive mode) calculated mass for $C_{252}H_{370}N_{74}O_{70}$: 5555.8; found: 5556.2.

2.5 Conjugate 1

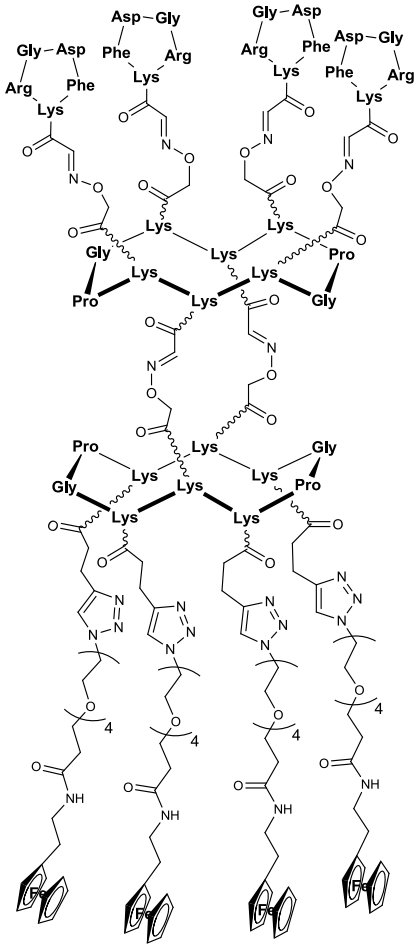

RP-HPLC profile and ESI-MS analysis of 1

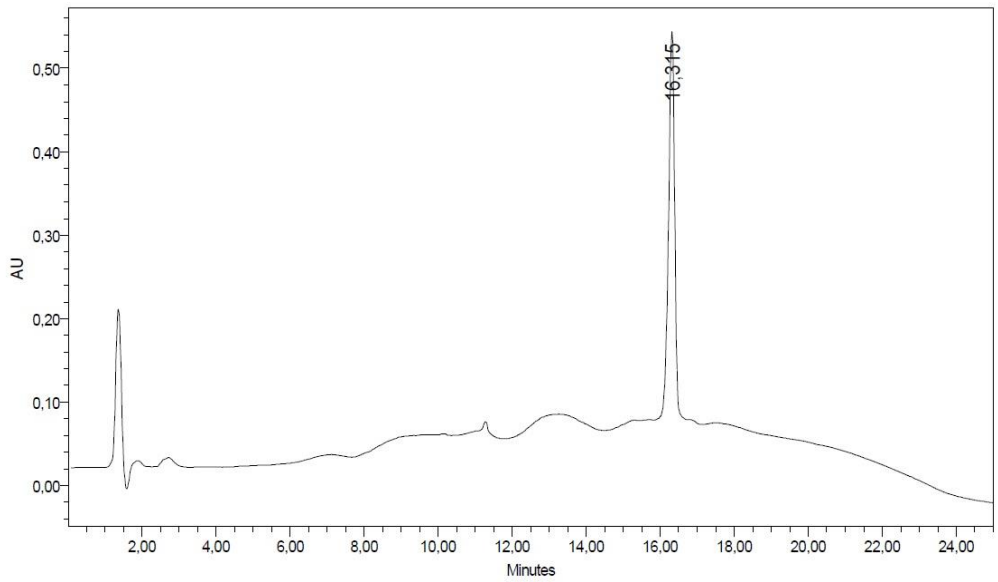

Figure S9: RP-HPLC profile of **1**.

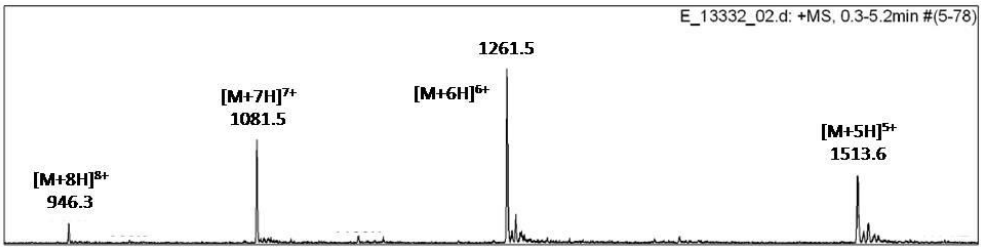

Figure S10: ESI-MS analysis of **1**.

Mass spectrum (ESI, positive mode) calculated mass for $C_{344}H_{506}Fe_4N_{90}O_{90}$: 7565.5; found: 7564.3.

2.6 Conjugate 3

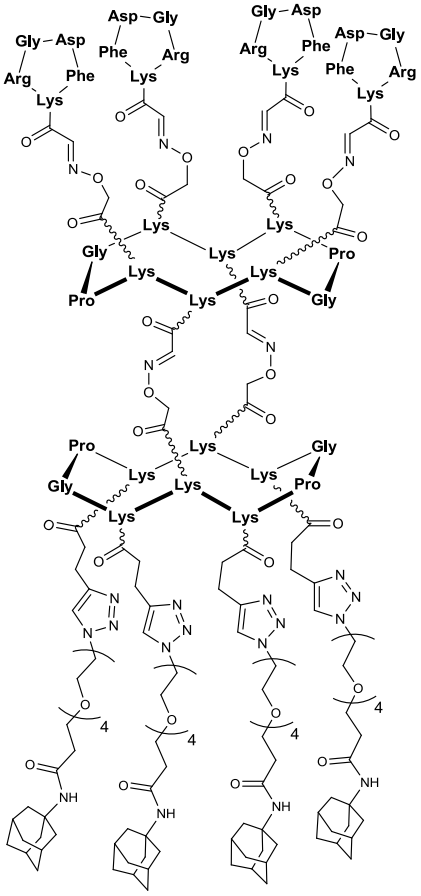

RP-HPLC profile and ESI-MS analysis of 3

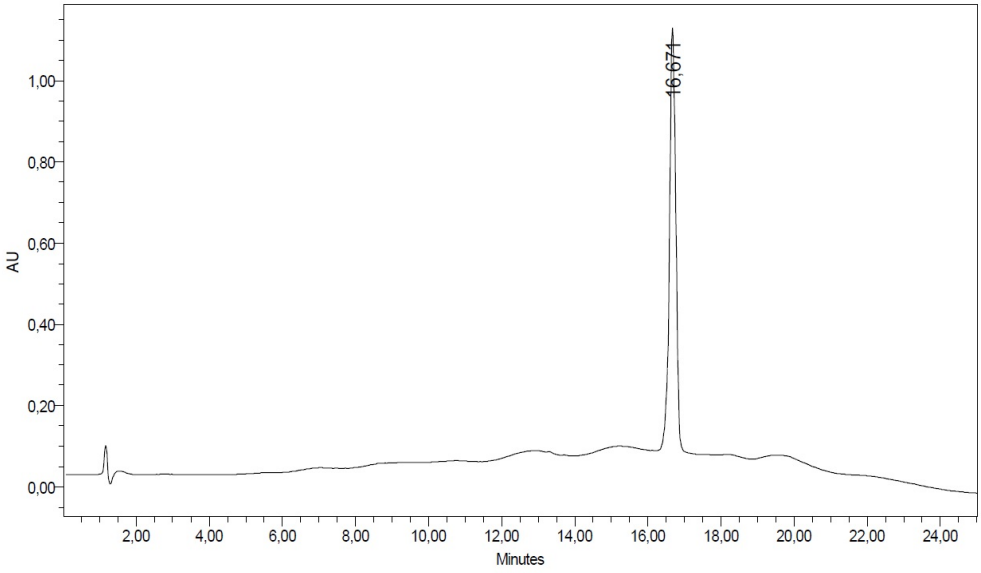

Figure S11: RP-HPLC profile of **3**.

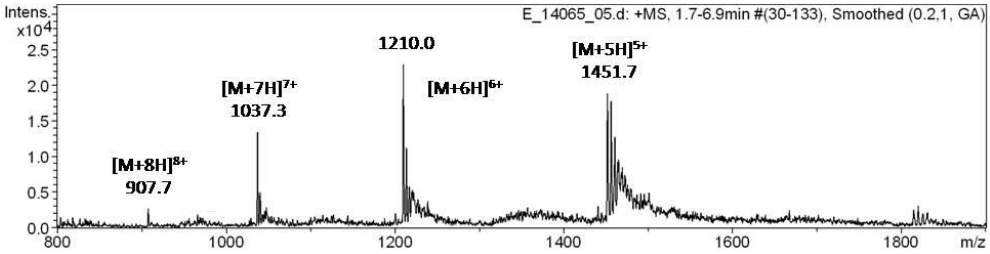

Figure S12: ESI-MS analysis of **3**.

Mass spectrum (ESI, positive mode) calculated mass for $C_{336}H_{514}N_{90}O_{90}$: 7254.2; found: 7254.8.

2.7 Conjugate 4

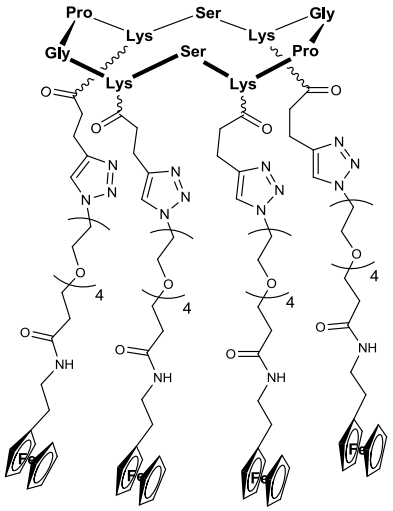

Compound **4** was prepared according to a strategy described earlier.[i]

RP-UHPLC profile and ESI-MS analysis of 4

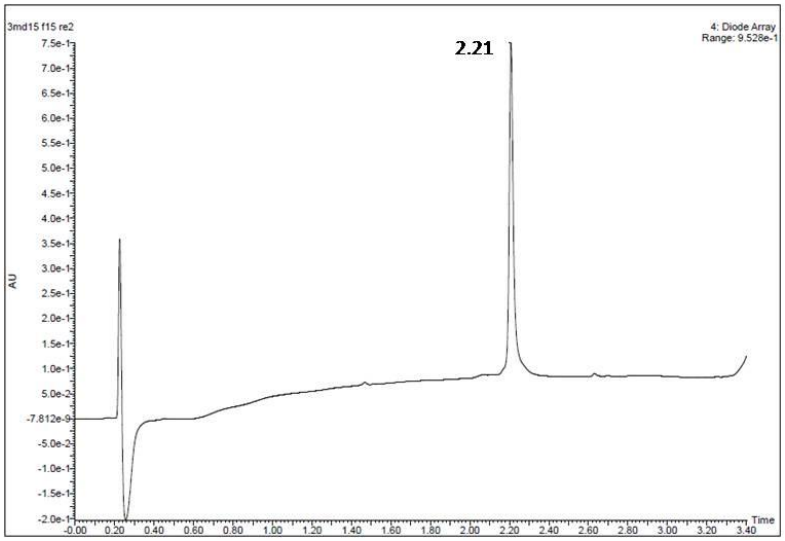

Figure S13: RP-UHPLC profile of **4**.

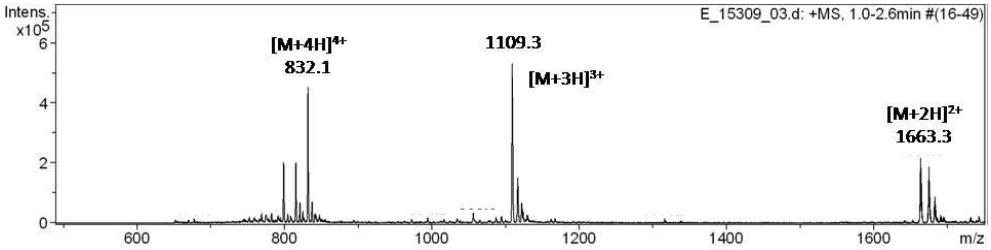

Figure S14: ESI-MS analysis of **4**.

Mass spectrum (ESI, positive mode) calculated mass for $C_{156}H_{230}Fe_4N_{30}O_{36}$: 3324.5; found: 3323.7.

3. Supplementary QCM-D data and quantification of adsorbed compound 1, 2 and 4

3.1 Absence of non-specific adsorption of compound 1 on oligoethylene glycol functionalized SAM surface

QCM-D profile presented in the Figure S15 demonstrates the absence of non-specific adsorption of compound **1** on an oligoethylene glycol functionalized SAM surface (prepared by overnight immersion of gold surfaces in pure HS-$(CH_2)_{11}$-EG_4-OH at 1mM in ethanol).

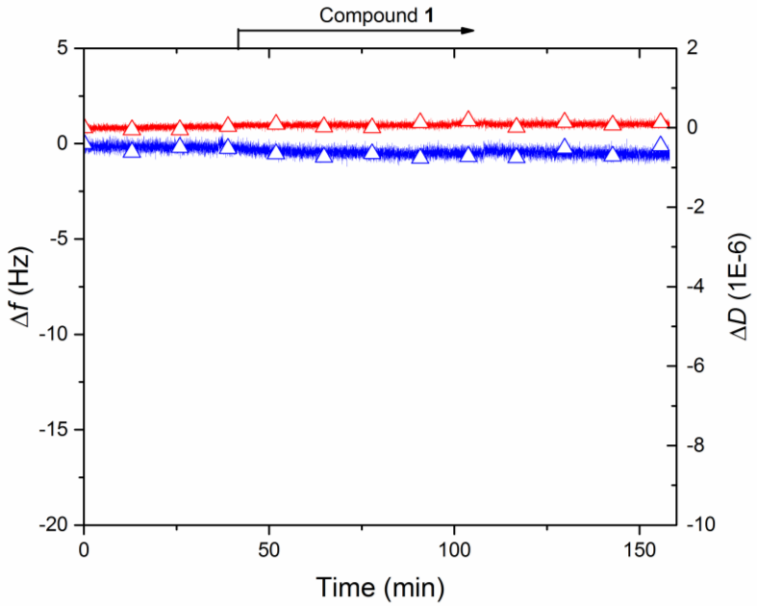

Figure S15: QCM-D profile (frequency shift – blue, dissipation shift – red) demonstrating the absence of non-specific adsorption of compound **1** on an oligoethylene glycol functionalized SAM surface lacking β-CD (compound **1** was injected at a concentration of 0.8 µM in PBS). Conditions: T = 24°C, flow rate = 20 µL.min^{-1}. The arrow on top of the graph indicates the start and duration of sample incubation. Before sample incubation, and after saturated binding, the surface was exposed to pure running buffer (PBS).

3.2 Quantification of RGD surface densities

RGD surface densities in mixed peptide derivative monolayers

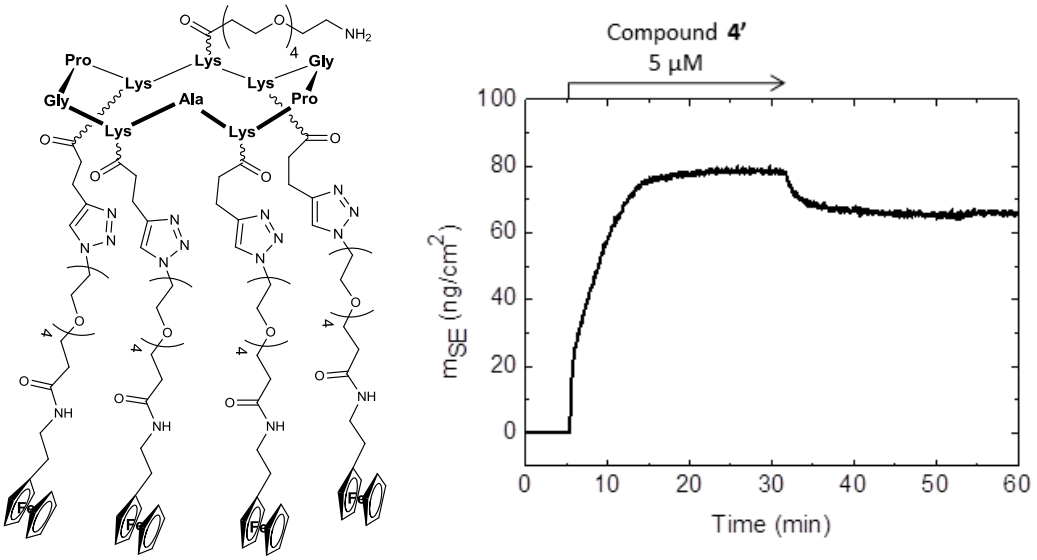

Figure S16: Structure and areal mass density of compound **4'** (the structure of this compound is analogous to the compound **4**; *M* = 3773.6 Da) determined by SE. Start and duration of injection of **4'** (5 µM) is indicated by an arrow. Before sample incubation, and after saturated binding, the surface was exposed to pure running buffer (PBS). The surface density of **4'** stably bound after rinsing was 18.6 ± 1.0 pmol/cm^2.

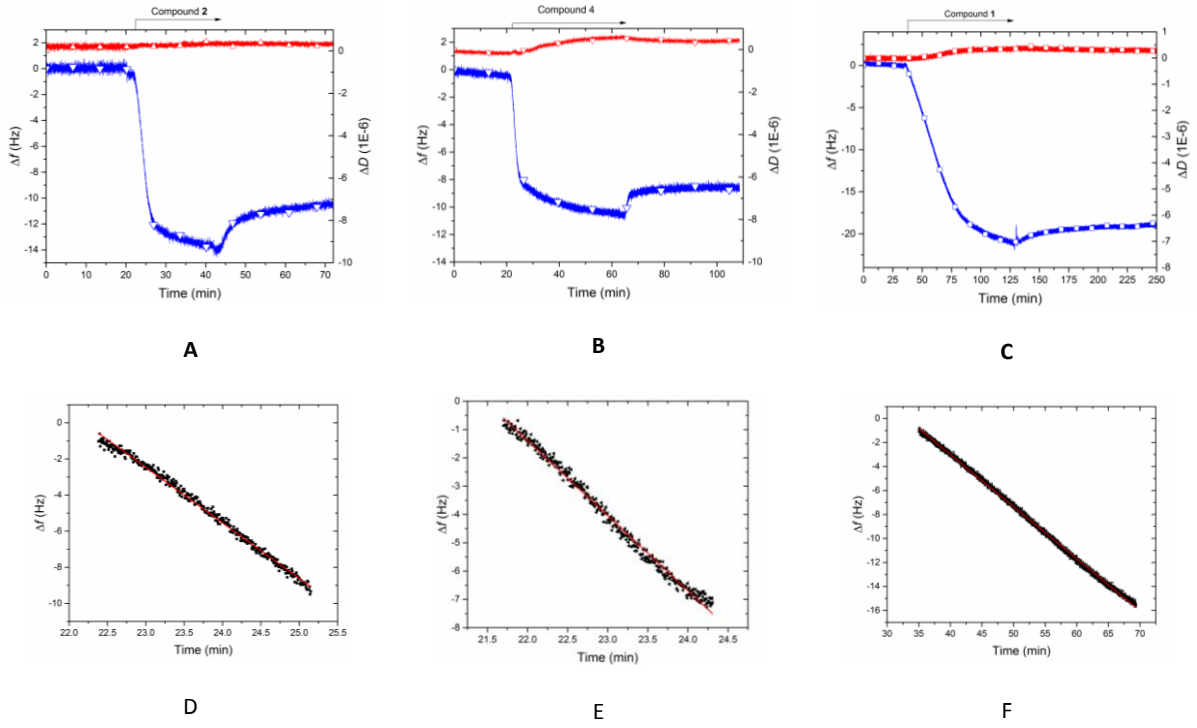

Figure S17: (A-C) QCM-D signals (frequency shifts – blue, dissipation shifts – red) recorded during the adsorption of 3.3 µM compound **2** (A) or 2.5 µM compound **4** (B) and 0.8 µM compound **1** (C). The arrows represent the start and duration of sample injections. T = 24°C, flow rate = 20 µL.min^{-1}. (D-F) Linear parts of binding curves (black dots) with linear fits (red lines) for compound **2** (D; data from A), **4** (E; data from B) and **1** (F; data from Figure 3). The frequency response rates d*f*/d*t* corresponding to the slopes of the fits are given in Table 1.

4. Optical micrographs of cell adhesion on surfaces displaying compound 1 or 2.

All optical imaging was performed on QCM-D sensors functionalized with β-CD SAM and installed in the Q-Sense Window Module, with 5000 cells/mL injected for 3 min at 100 µL/min in DMEM, unless otherwise stated.

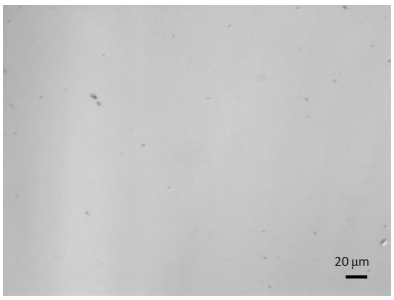

Figure S18: HEK-293(β3) cells on 100% compound **4**. No cells are observed, confirming surface passivation. The image is representative of the entire surface.

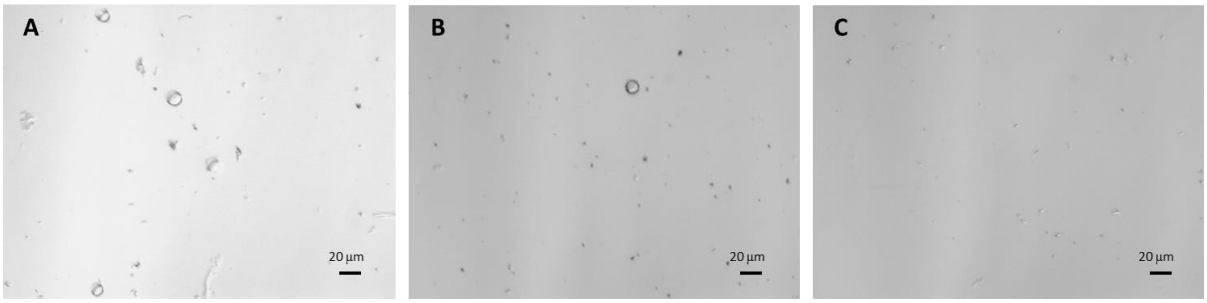

Figure S19: (A) HEK-293(β3) cells on 100% compound **1**; (B) HEK-293(β3) cells on 100% compound **2**; (C) HEK-293(β1) cells on 100% compound **1**. The images are representative of the entire surfaces, a few cells per field of view are typically observed.

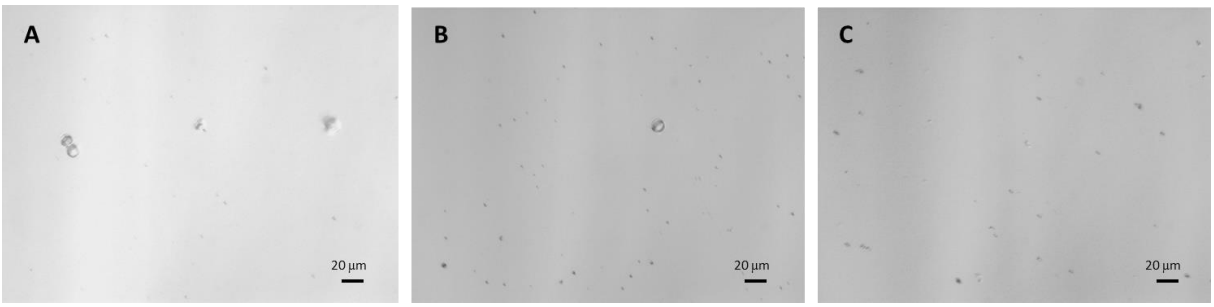

Figure S20: (A) HEK-293(β3) cells on 0.95% compound **1**; (B) HEK-293(β3) cells on 1.0% compound **2**; (C) HEK-293(β1) cells on 0.95% compound **1**.

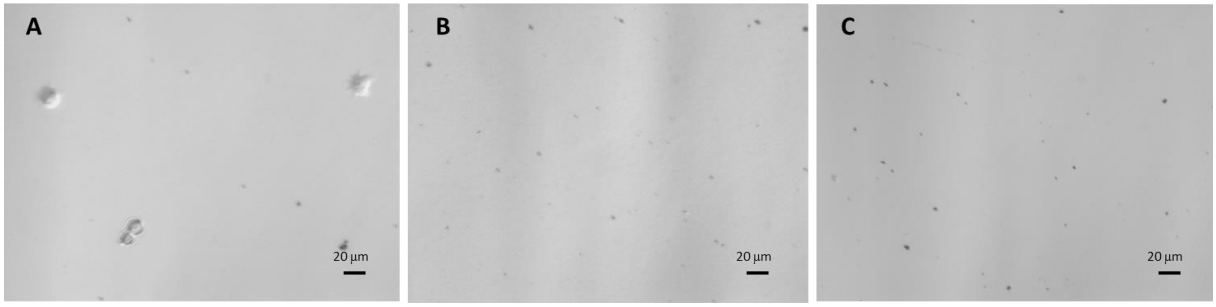

Figure S21: (A) HEK-293(β3) cells on 0.084% compound **1**; (B) HEK-293(β3) cells on 0.10% compound **2**; (C) HEK-293(β1) cells on 0.084% compound **1**.

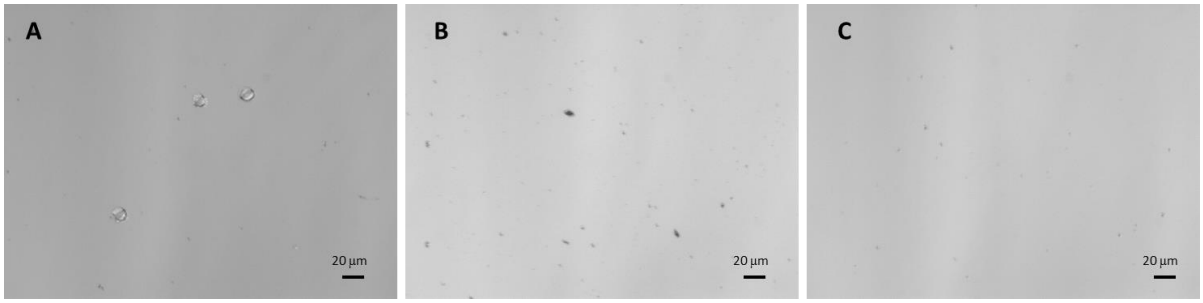

Figure S22: (A) HEK-293(β3) cells on 0.0084% compound **1**; (B) HEK-293(β3) cells on 0.00084% compound **1**; (C) HEK-293(β1) cells on 0.0084% compound **1**.

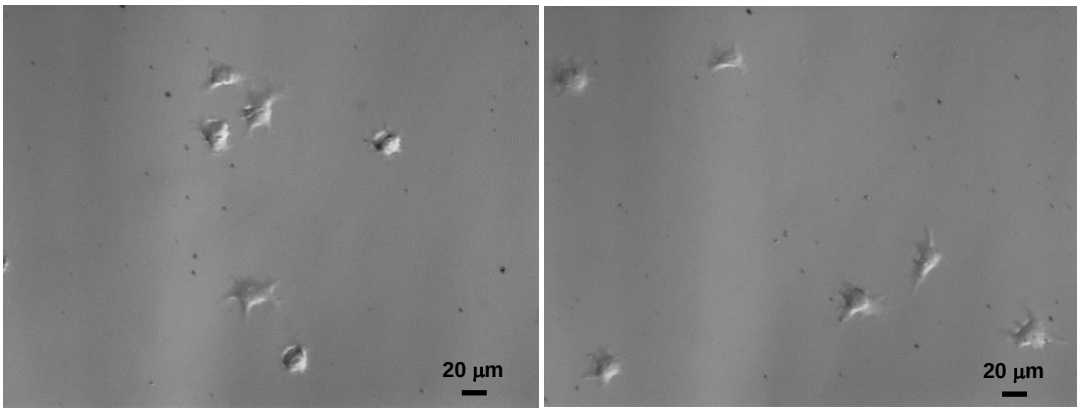

Figure S23: HEK-293(β3) cells on 0.0084% compound **1** 20 min after cell injection.

5. Electrochemical release of RGD compounds

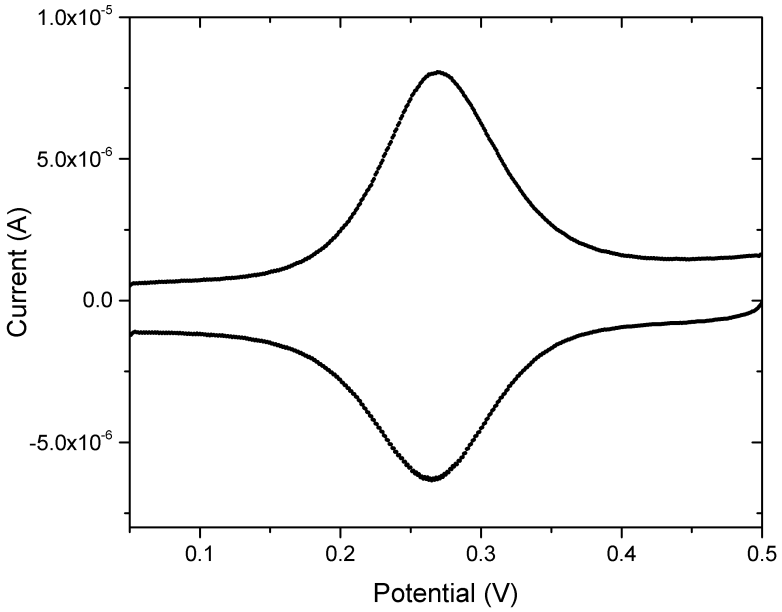

Figure S24: Cyclic voltammogramm (CV) recorded on gold quartz crystal (QCM-D gold sensor, gold disk diam. 1.1 cm) coated with β-CD SAM functionalized with compound **2** in 0.1 mol. L^{-1} KPF_6 aqueous electrolyte (without compound **2** in solution) (γ = 100mV s^{-1}). The CV curve characterized the electrochemical response of Fc encapsulated in β-CD cavity. The observed peak-to-peak potential splitting (5 mV at 100 mV/s) indicates that the voltametric response arises from surface immobilized Fc. We noticed that the reduction peak current (6.3 μA) is lower than the oxidation one (8 μA). This behavior can be explained by the dissociation of the inclusion complex during the Fc oxidation, Fc is converted to Fc^{+} and the Fc-β-CD interaction is broken. Thus, on the reverse sweep less Fc are available for the reduction of Fc^{+} to Fc (a lower ratio of inclusion complex were restored), because some of Fc compound **2** diffused in the solution. During the time scale of the potential sweep (100 mV/s) the ratio of compound 2 loosed in solution is low. For this electrochemical experiment KPF_6 has been selected because of the lipophilic properties of the PF_6^- anion that facilitates the charge compensation during the electrochemical oxidation of the hydrophobic Fc moieties. In reverse the oxidation of Fc-βCD inclusion complex in PBS buffer solution leads to distorted CV curve and the oxidation requires higher potential, that is the reason of 0.55V applied potential.

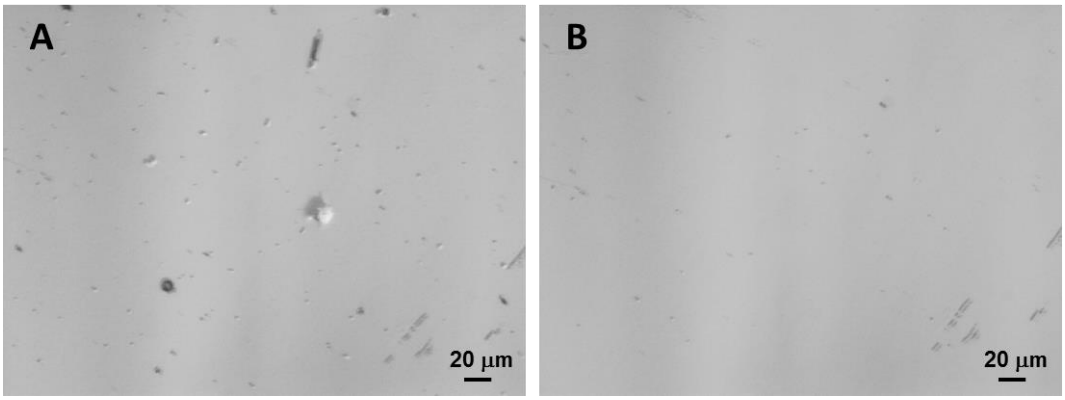

Figure S25: Electrochemical detachment assay on HEK-293(β3) cells on 0.0084% compound **1**. Micrographs (A) was taken after cell injection for 3 min. Micrographs (B) was taken on the same spots after applying an oxidative potential (0.55 V vs. AgCl/Ag), gentle rinsing of the surfaces with DMEM outside the measurement chamber and replacing in the QCM-D module for imaging.

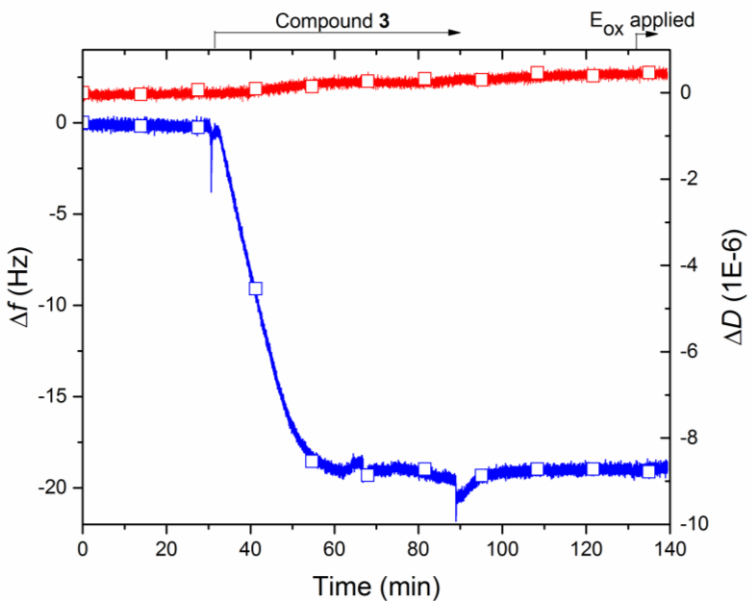

Figure S26: Binding of compound **3** (2 µM) to a β-CD SAM and lack of electrochemical release. QCM-D (frequency shifts – blue, dissipation shifts – red) is combined with electrochemistry. Compound **3** is not released by the potential of 0.55 V *vs.* AgCl/Ag, confirming that the AD guest layer is not sensitive to the oxidative potential. The arrows represent the start and duration of sample injection and application of oxidative potential; T = 24°C, flow rate = 20 µL.min^{-1}.

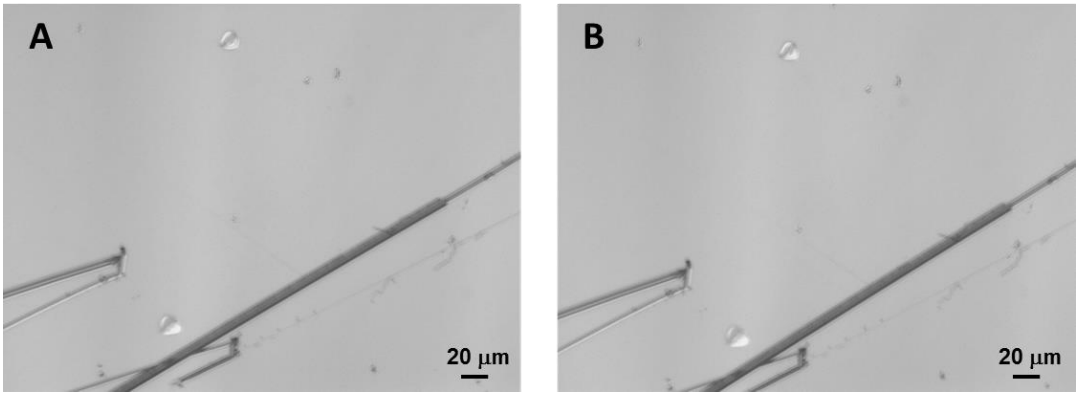

Figure S27: Electrochemical detachment assay on HEK-293(β3) cells on 100% compound **3**. Micrograph (A) was taken after cell injection for 3 min. Micrograph (B) was taken on the same spot after the same treatment as for Figures S25B.

Supplementary reference

[i] D. Thakar, L. Coche-Guérente, M. Claron, C. H. F. Wenk, J. Dejeu, P. Dumy, P. Labbé and D. Boturyn, *ChemBioChem* 2014, **15**, 377.